Supplementary Information

AIG1 and ADTRP are Atypical Integral Membrane Hydrolases that Degrade Bioactive FAHFAs

William H Parsons[1#], Matthew J Kolar[2#], Siddhesh S Kamat[1], Armand B Cognetta III[1], Jonathan J Hulce[1], Enrique Saez[1,^], Barbara B Kahn[3,^], Alan Saghatelian[2,^,*], Benjamin F Cravatt[1,^,*]

[1]The Skaggs Institute for Chemical Biology, Department of Chemical Physiology, The Scripps Research Institute, La Jolla, CA 92037; [2]Salk Institute for Biological Studies, Clayton Foundation Laboratories for Peptide Biology, Helmsley Center for Genomic Medicine, La Jolla, California 92037, United States; [3]Division of Endocrinology, Diabetes & Metabolism, Department of Medicine, Beth Israel Deaconess Medical Center and Harvard Medical School, Boston, Massachusetts 02215, United States

#These authors contributed equally to this work

^Co-senior authors

Supplementary Results

Table of Contents

Supplementary Figures 1−18 3−28

Supplementary Tables 1−4 29-32

- See also separate Excel files for **Supplementary Tables 1** and **2**

References 33

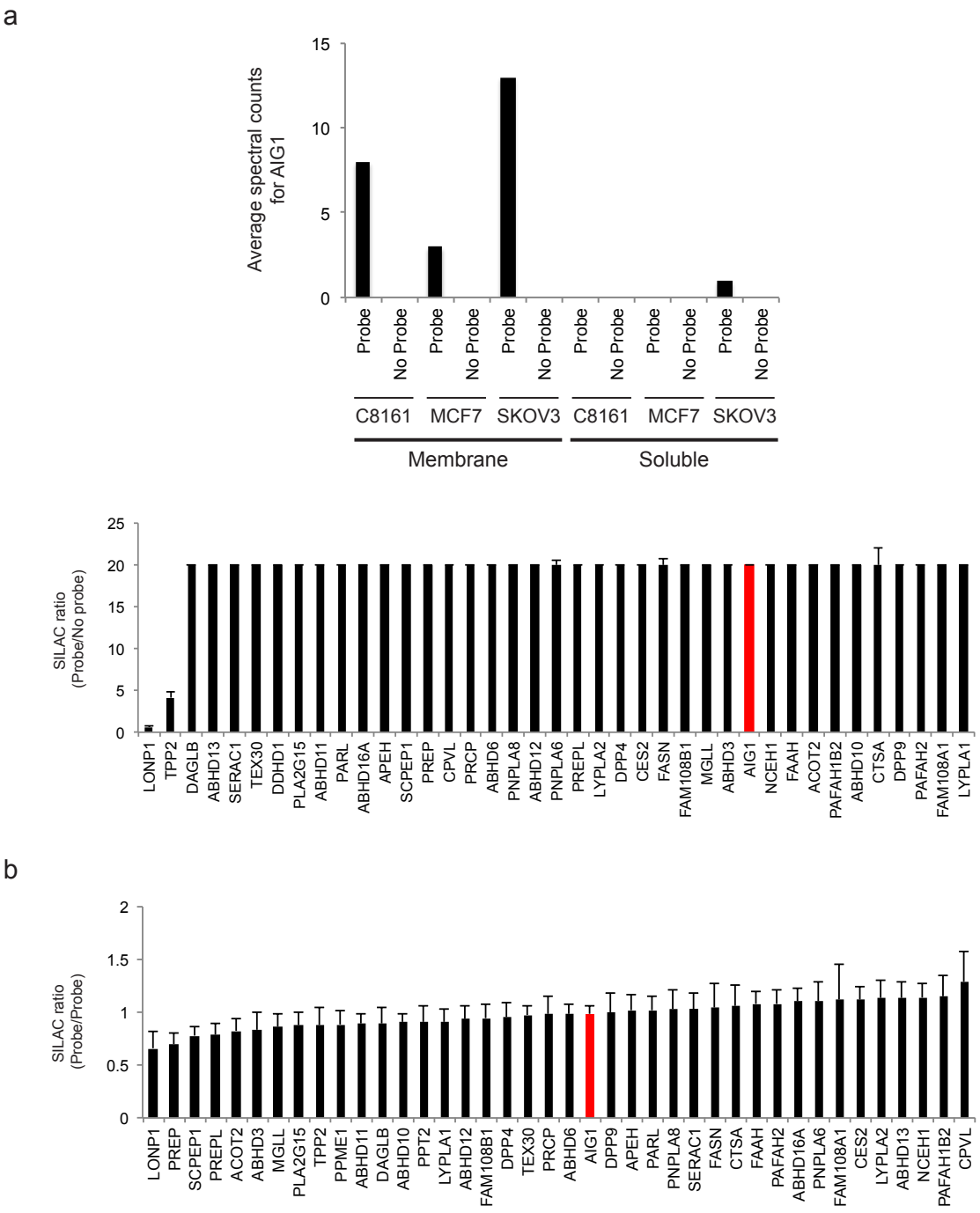

Supplementary Fig. 1. Additional analysis of AIG1 signals in MS-based ABPP experiments. (**a**) Upper graph, mean spectral count values for AIG1 in previous ABPP-MudPIT experiments performed on human cancer cell lines using the FP-biotin probe. These data were extracted from reference 1 and show enrichment of AIG1 from FP-

biotin, but not no-probe control experiments performed with cancer cell membrane proteomes. Lower graph, ABPP-SILAC analysis of a control experiment comparing proteins from heavy amino acid-labeled SKOV3 cell proteome treated with FP-biotin (5 μM) with proteins from an untreated light amino acid-labeled SKOV3 cell proteome, confirming enrichment of the Ser hydrolases identified in **Fig. 1a** (including AIG1). Data represent the median SILAC ratios ± s. d. for peptides quantified for each protein from two biological replicates. (**b**) ABPP-SILAC analysis of a control experiment comparing FP-biotin-enriched proteins from heavy and light amino acid-labeled SKOV3 cell proteomes each treated with the same concentration of FP-biotin (5 μM), confirming a SILAC ratio of ~1.0 for the Ser hydrolases identified in **Fig. 1a** (including AIG1). Data represent the median SILAC ratios ± s. d. for peptides quantified for each protein from two biological replicates.

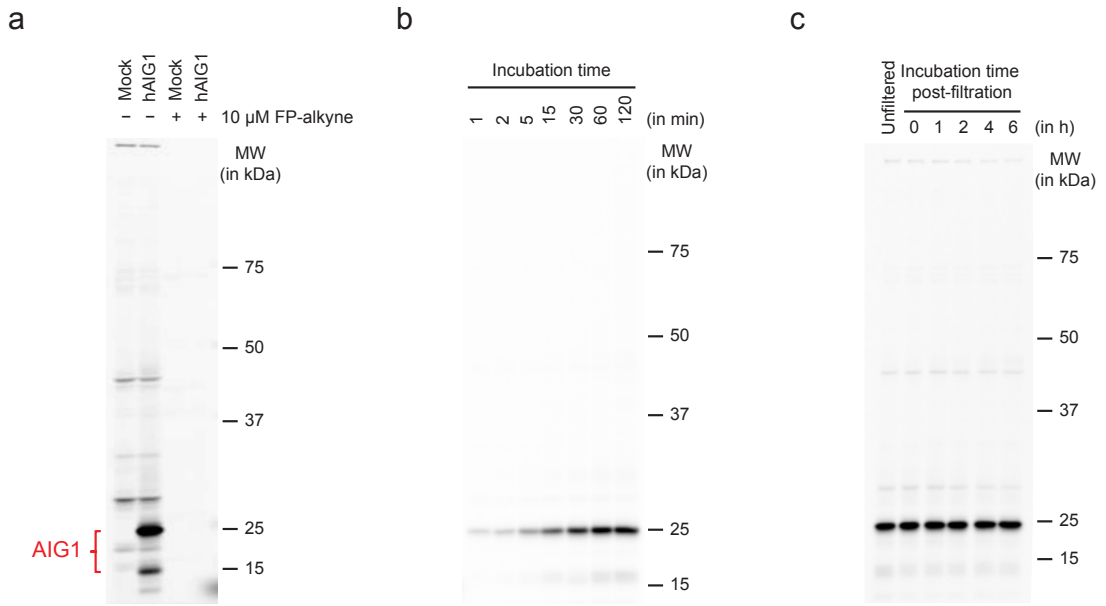

Supplementary Fig. 2. Characterization of FP-reactivity of recombinant hAIG1. (**a**) ABPP gel of the membrane proteomes (1.0 mg proteome mL^{-1}) of mock- and hAIG1-transfected HEK293T cells showing FP-labeling of AIG1. Proteomes were treated with either DMSO or FP-alkyne for 30 min at 37 °C, followed by FP-rhodamine (1 μM, 30 min, 37 °C). (**b**) ABPP gel of the membrane proteome (0.5 mg proteome mL^{-1}) of hAIG1-transfected HEK293T cells showing time course of FP labeling. Proteomes were treated with 1 μM FP-Rh at 37 °C for the indicated time. (**c**) ABPP gel of the membrane proteome (0.5 mg proteome mL^{-1}) of hAIG1-transfected HEK293T cells showing irreversibility of FP labeling. Proteome was treated with FP-rhodamine (1 μM, 30 min, 37 °C) and, following gel filtration to remove excess probe, samples were incubated at 37 °C for the indicated time before SDS-PAGE and in-gel fluorescence scanning.

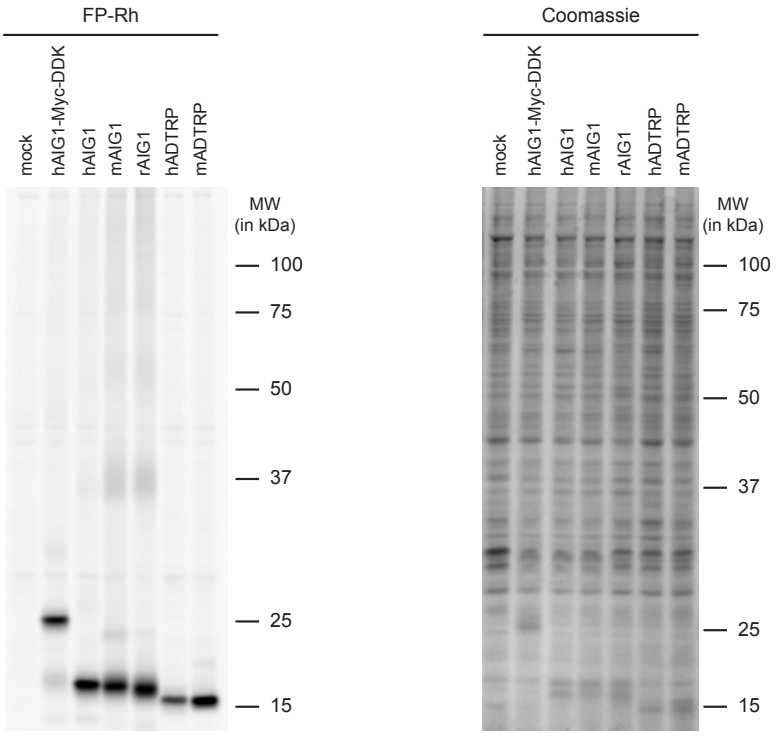

Supplementary Fig. 3. AIG1 and ADTRP orthologues also react with FP probes. *Left image*, ABPP gel of the membrane proteomes (0.5 mg proteome mL^{-1}) of mock-, C-terminal-tagged hAIG1-, and untagged hAIG1-, mouse (m)AIG1-, rat (r)AIG1-, hADTRP-, and mADTRP-transfected HEK293T cells demonstrating labeling of all variants by FP-Rh. Proteomes were treated with 1 μM FP-Rh for 30 min at 37 °C and analyzed by SDS-PAGE and in-gel fluorescence scanning. *Right image*, Coomassie blue-stained gel to assess relative protein expression (right gel).

a

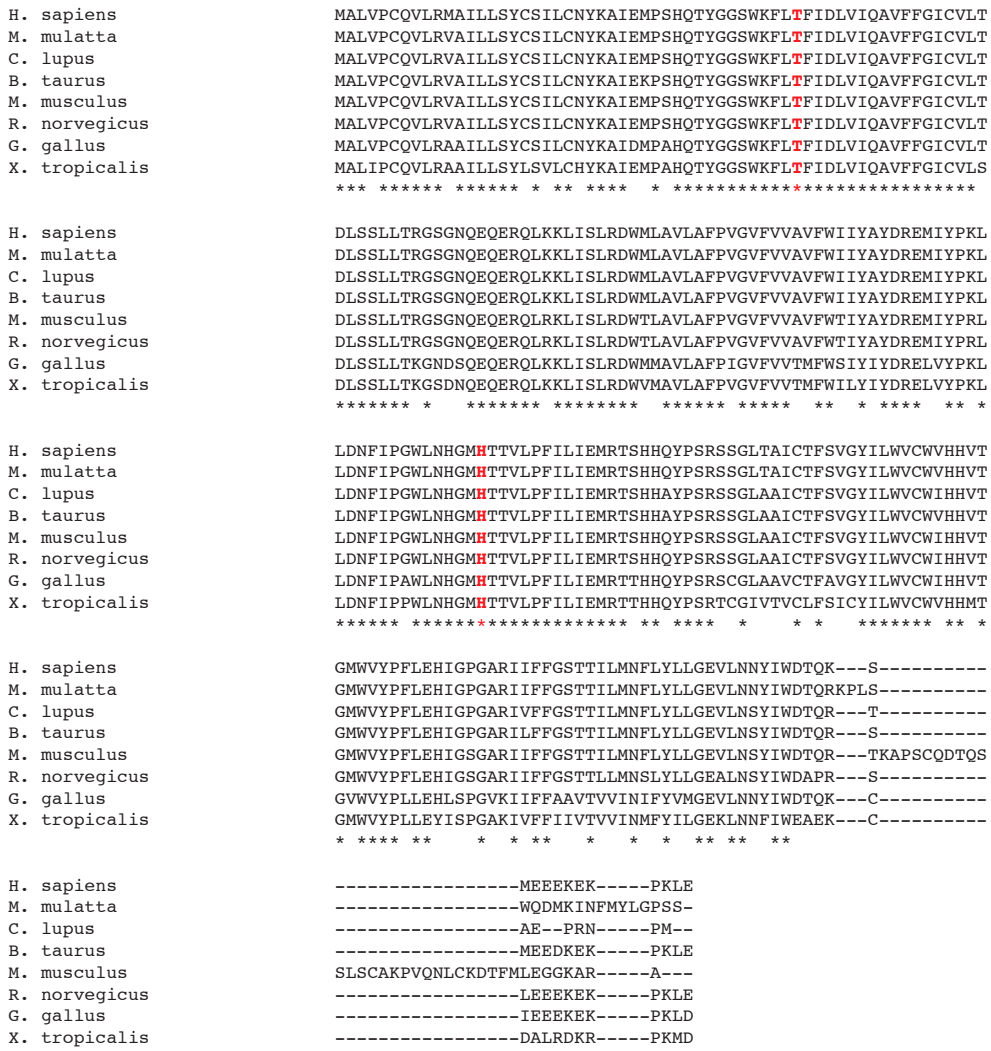

b

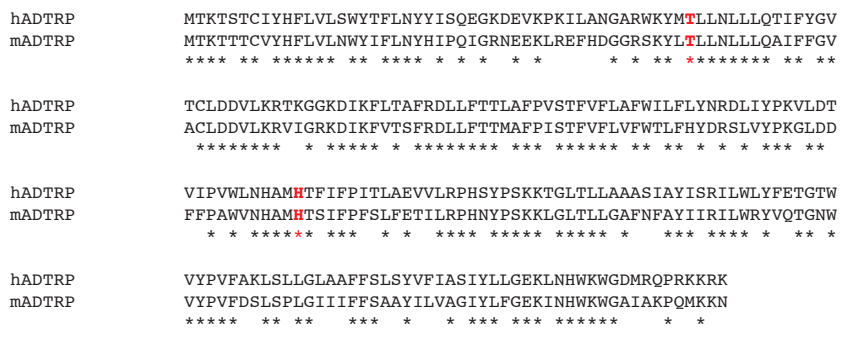

Supplementary Fig. 4. Additional sequence alignments of AIG1 and ADTRP proteins from different species. (**a**) Sequence alignment of AIG1 orthologues across multiple

species (http://www.st-va.ncbi.nlm.nih.gov/tools/cobalt/cobalt.cgi). Asterisks indicate residues conserved across all of the displayed proteins; the proposed Thr nucleophile and His base are shown in red. (**b**) Sequence alignment of mouse and human ADTRP (http://www.st-va.ncbi.nlm.nih.gov/tools/cobalt/cobalt.cgi). Asterisks indicate residues conserved between the two sequences; the proposed Thr nucleophile and His base are shown in red.

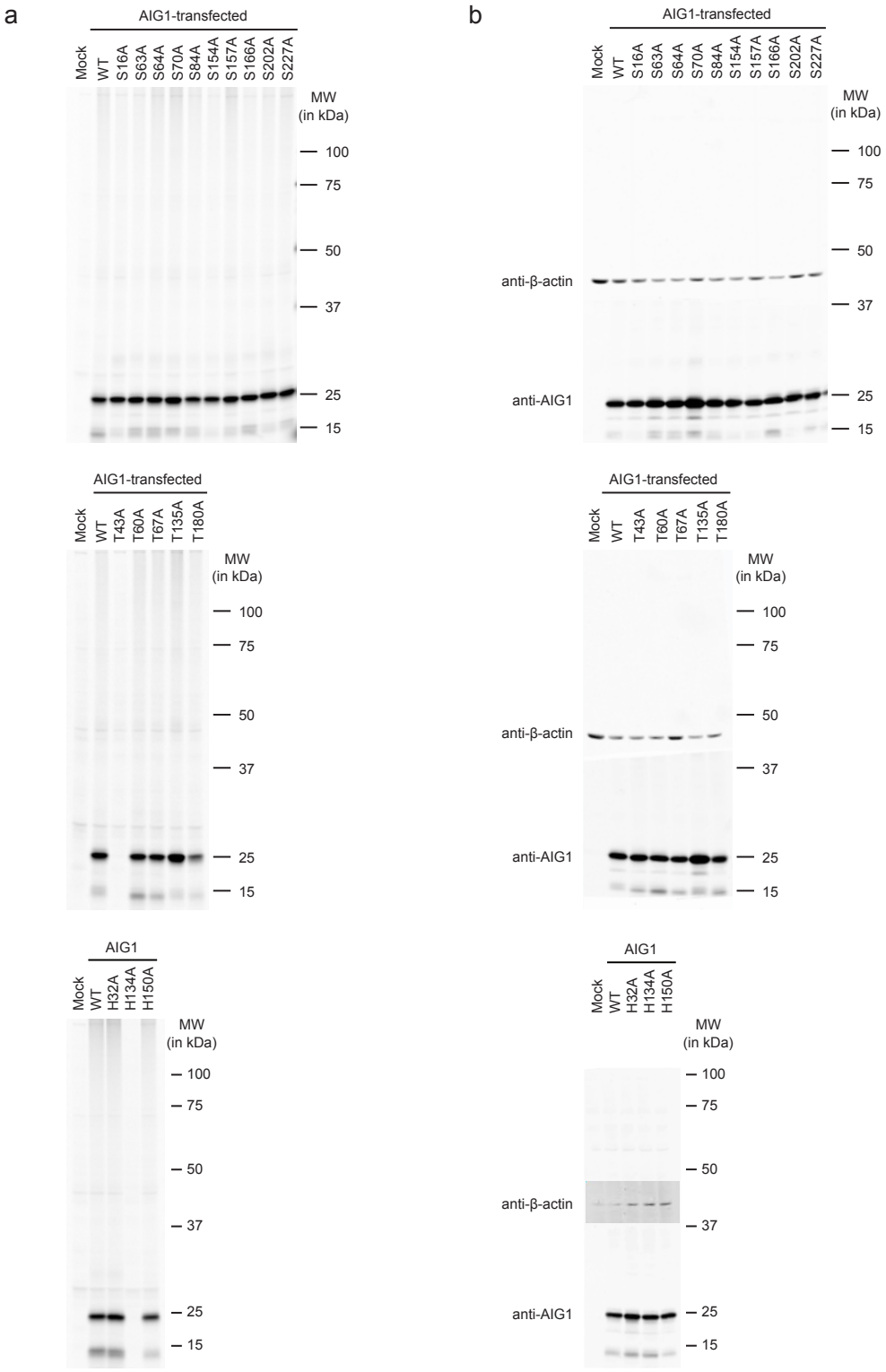

Supplementary Fig. 5. Assessment of FP reactivity of hAIG1 Ser, Thr, and His mutants.

(**a**) ABPP gels of membrane proteomes (0.5 mg proteome mL^{-1}) of mock-, wild-type

hAIG1-, and mutant hAIG1-transfected HEK293T cells. Proteomes were treated with 1 μM FP-Rh for 30 min at 37 °C and analyzed by SDS-PAGE and in-gel fluorescence scanning. (**b**) Western blots of membrane proteomes (0.5 mg proteome mL^{-1}) of mock-, wild-type hAIG1-, and mutant hAIG1-transfected HEK293T cells. β-actin was measured as a loading control.

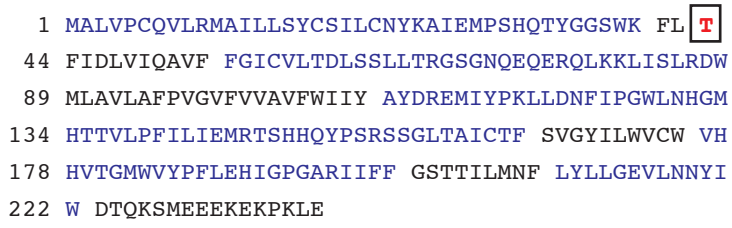

Supplementary Fig. 6. Sequence coverage of hAIG1 enriched and characterized from transfected HEK293T cells using ABPP-MudPIT and ABPP-SILAC experiments with the FP-biotin probe. Portions of the hAIG1 sequence observed by LC-MS are colored in blue; Thr43 is boxed and colored red.

a

Program	TM1	TM2	TM3	TM4	TM5	TM6
Uniprot	1-21	39-59	88-108	124-144	167-187	197-217
Tmpred	3-27	41-59	88-112	124-143	161-184	194-213
PSORT II	6-22	42-58	92-108	——	158-174	197-213
TMHMM	13-30	45-67	88-110	125-144	157-179	194-216
Phobius	7-27	47-67	88-108	128-147	159-185	197-217
CCTOP	8-27	44-66	88-110	127-145	158-177	194-214

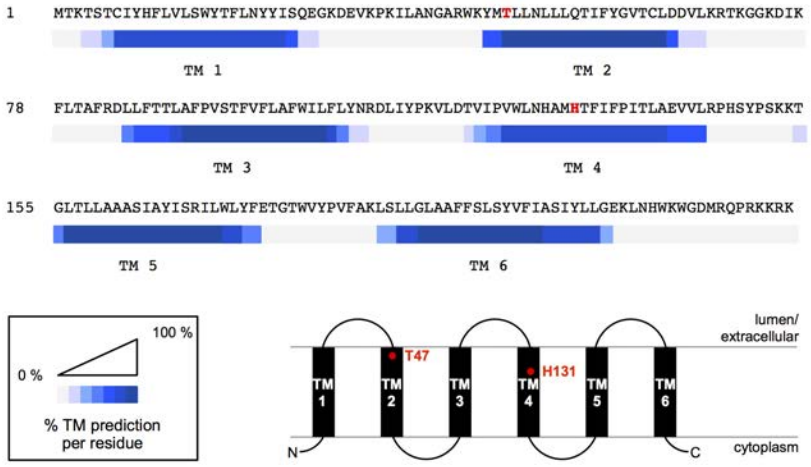

b

Program	TM1	TM2	TM3	TM4	TM5	TM6
Uniprot	4-24	47-67	86-106	120-140	155-175	190-210
Tmpred	6-25	45-63	91-109	121-144	156-175	190-211
PSORT II	——	47-63	90-106	——	155-171	188-204
TMHMM	7-25	45-64	85-107	122-144	156-173	188-210
Phobius	7-25	45-64	85-105	125-144	156-175	190-210
CCTOP	7-27	45-64	85-107	125-144	154-173	192-211

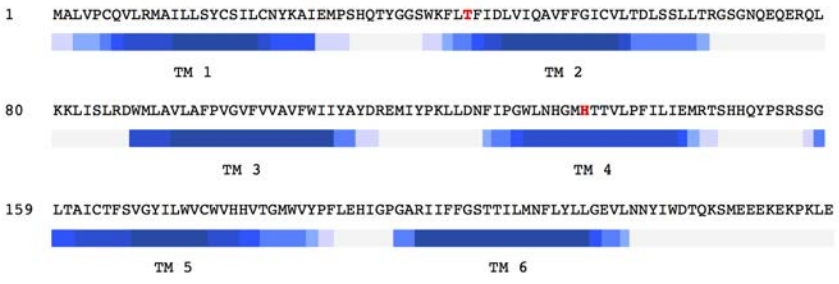

Supplementary Fig. 7. Predicted transmembrane domains and topology of AIG1 and ADTRP. Predicted transmembrane domains and topology maps for AIG1 (**a**) and ADTRP (**b**) based on six different transmembrane topology prediction programs

(CCTOP, Phobius, PSORT II, TMHMM, TMpred, and Uniprot). Each table entry represents the span of residues in the protein sequence predicted to be transmembrane-embedded by the indicated program. Five of the six programs predict six transmembrane domains (TM1 through TM6) for AIG1 and ADTRP. In the topology maps, residues are color-coded based on the percentage of programs that predict localization in the membrane. Thr-43 and His-134 of AIG1 and Thr-47 and His-131 of ADTRP are indicated in red.

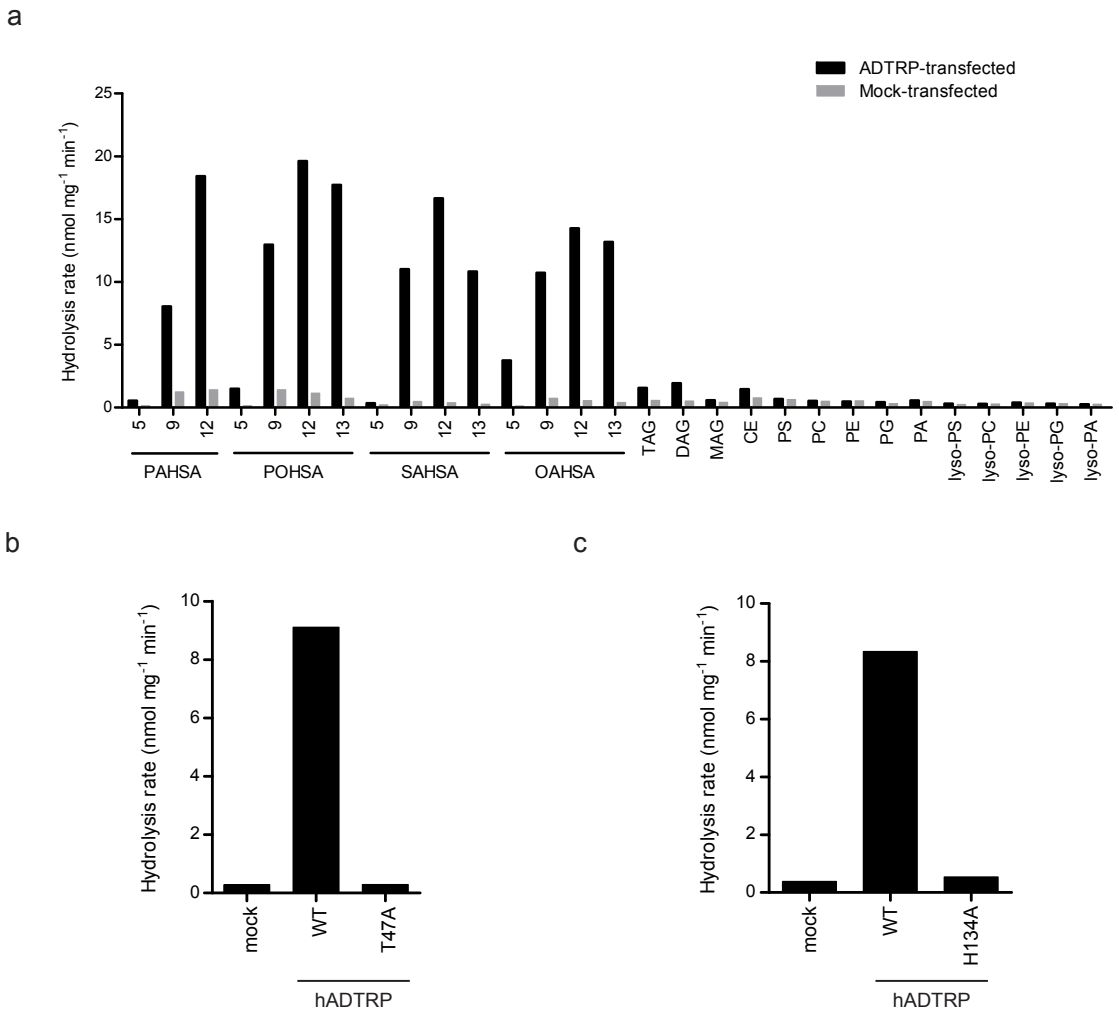

Supplementary Fig. 8. ADTRP shows FAHFA hydrolase activity. (**a**) *In vitro* lipid substrate hydrolysis assays for membrane proteomes of mock- and hADTRP-transfected HEK293T cells. See legend for **Figure 3** for definitions of lipid substrates. For each assay, 20 μg of mock or ADTRP-transfected proteome was incubated with 100 μM substrate for 30 min at 37 °C. Data represent mean values for two biological replicates. (**b** & **c**) *In vitro* 12-OAHSA hydrolysis assays for the membrane proteomes of mock, wild-type hADTRP, and T47A mutant hADTRP-transfected HEK293T cells. 20 μg of each proteome was incubated with 100 μM 12-OAHSA for 30 min at 37 °C. Data represent mean values for two biological replicates.

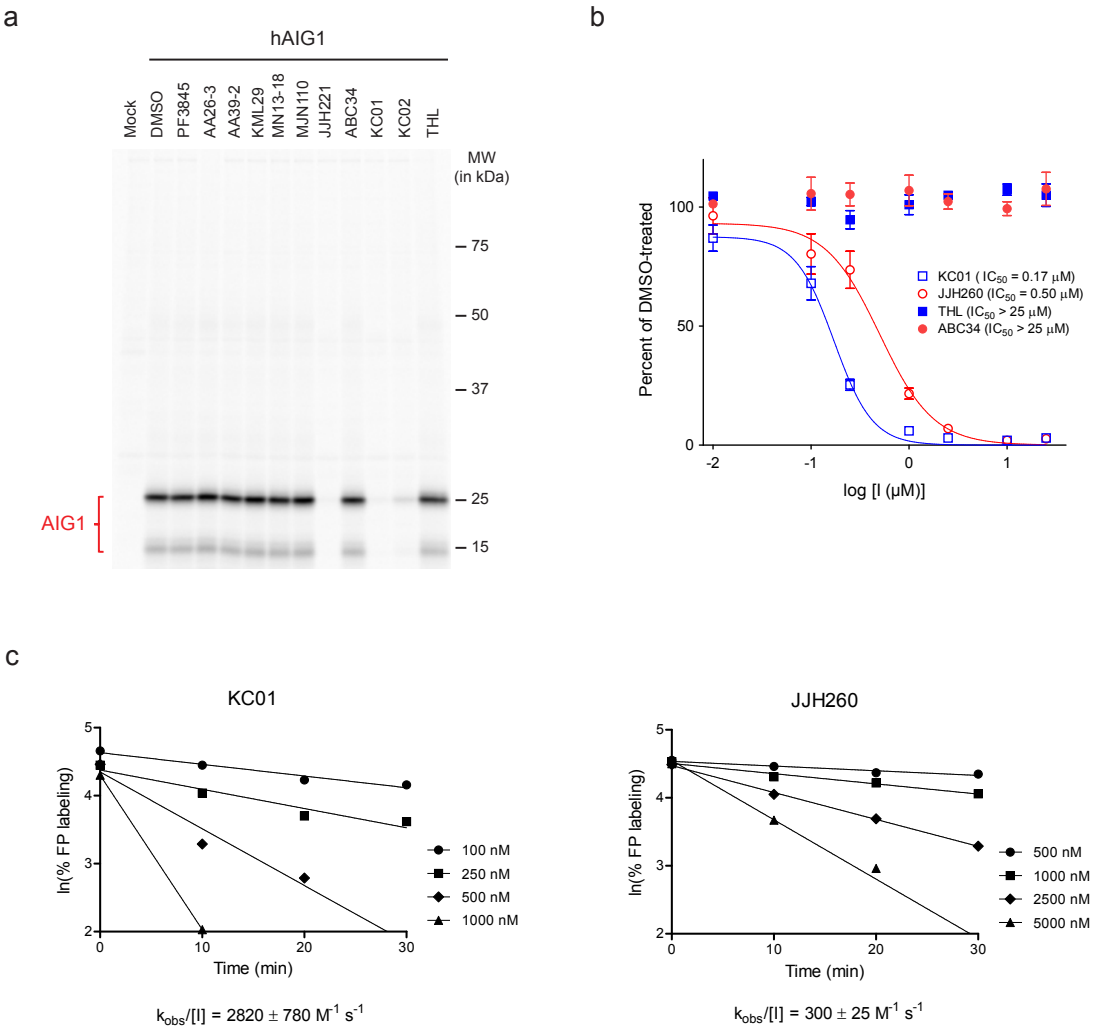

Supplementary Fig. 9. Evaluation of inhibitor sensitivity of AIG1 by competitive ABPP. (**a**) ABPP gel of the membrane proteome of hAIG1-transfected HEK293T cells (0.5 mg proteome mL^{-1}), treated with a collection of previously described Ser hydrolase inhibitors[2-6]. Proteomes were incubated with 20 μM inhibitor for 30 min at 37 °C and then treated with 1 μM FP-Rh for 30 min at 37 °C. (**b**) IC_{50} curves quantifying the inhibition of hAIG1 by KC01 (IC_{50} = 0.17 ± 0.03 μM) and JJH260 (IC_{50} = 0.50 ± 0.15 μM) as measured by gel-based competitive ABPP with the FP-Rh probe. Band intensities were quantified relative to the DMSO-treated control lane using ImageJ software

(http://imagej.nih.gov/ij/). Data represent mean values ± s. e. m. for three biological replicates. (**c**) Time-dependent inhibition of AIG1 by KC01 and JJH260 with calculated k_{obs}/[I] values as measured by competitive ABPP with the FP-Rh probe (1 μM, 2 min) following the indicated pre-treatment times with inhibitors. Data represent average values for three biological replicates; calculated k_{obs}/[I] values are expressed ± s. d.

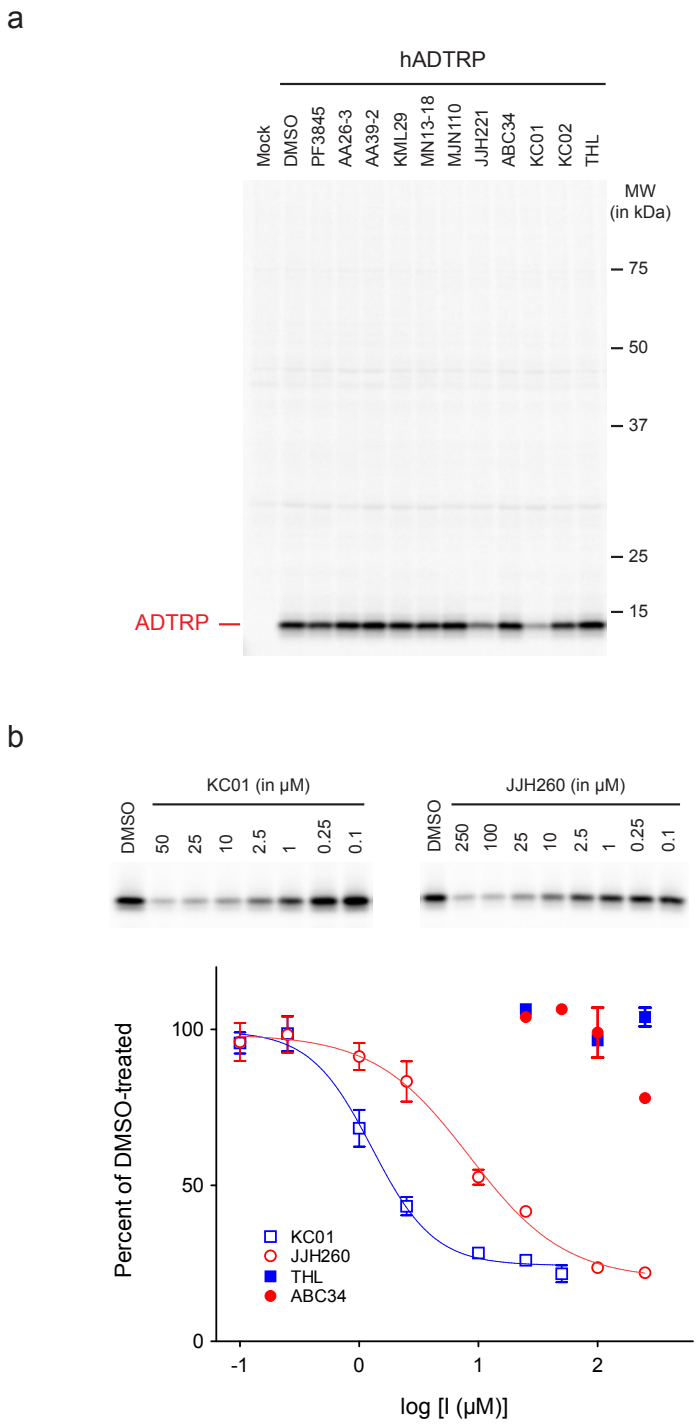

Supplementary Fig. 10. Evaluation of inhibitor sensitivity of ADTRP by competitive ABPP. (**a**) ABPP gel of the membrane proteome of hADTRP-transfected HEK293T cells

(0.5 mg proteome mL^{-1}), treated with a collection of previously described Ser hydrolase inhibitors[2-6]. Proteomes were incubated with 20 μM inhibitor for 30 min at 37 °C and then treated with 1 μM FP-Rh for 30 min at 37 °C. (**b**) IC_{50} curves quantifying the inhibition of hADTRP by KC01 (IC_{50} = 1.3 ± 0.4 μM) and JJH260 (IC_{50} = 8.5 ± 3.0 μM) as measured by gel-based competitive ABPP with the FP-Rh probe. Data represent average values ± s. e. m. for three biological replicates.

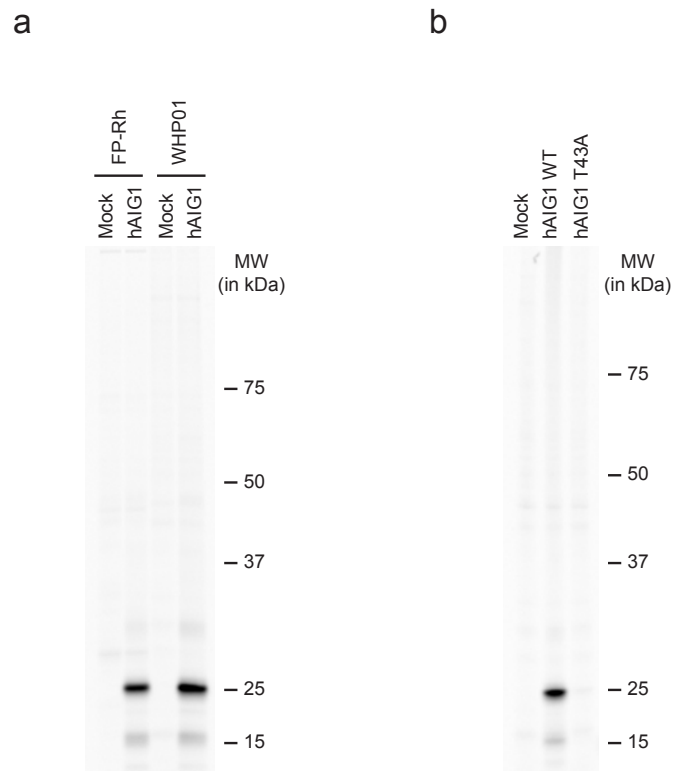

Supplementary Fig. 11. WHP01 labeling of AIG1. (**a**) ABPP gel of the membrane proteomes (0.5 mg proteome mL^{-1}) of mock- and hAIG1-transfected HEK293T cells, showing labeling of AIG1 by WHP01. Proteomes were treated with either 1 μM FP-Rh or 2 μM WHP01 for 30 min at 37 °C.. (**b**) ABPP gel of the membrane proteomes of mock-, wild-type hAIG1-, and mutant hAIG1-transfected HEK293T cells. Proteomes were treated with 2 μM WHP01 for 30 min at 37 °C.

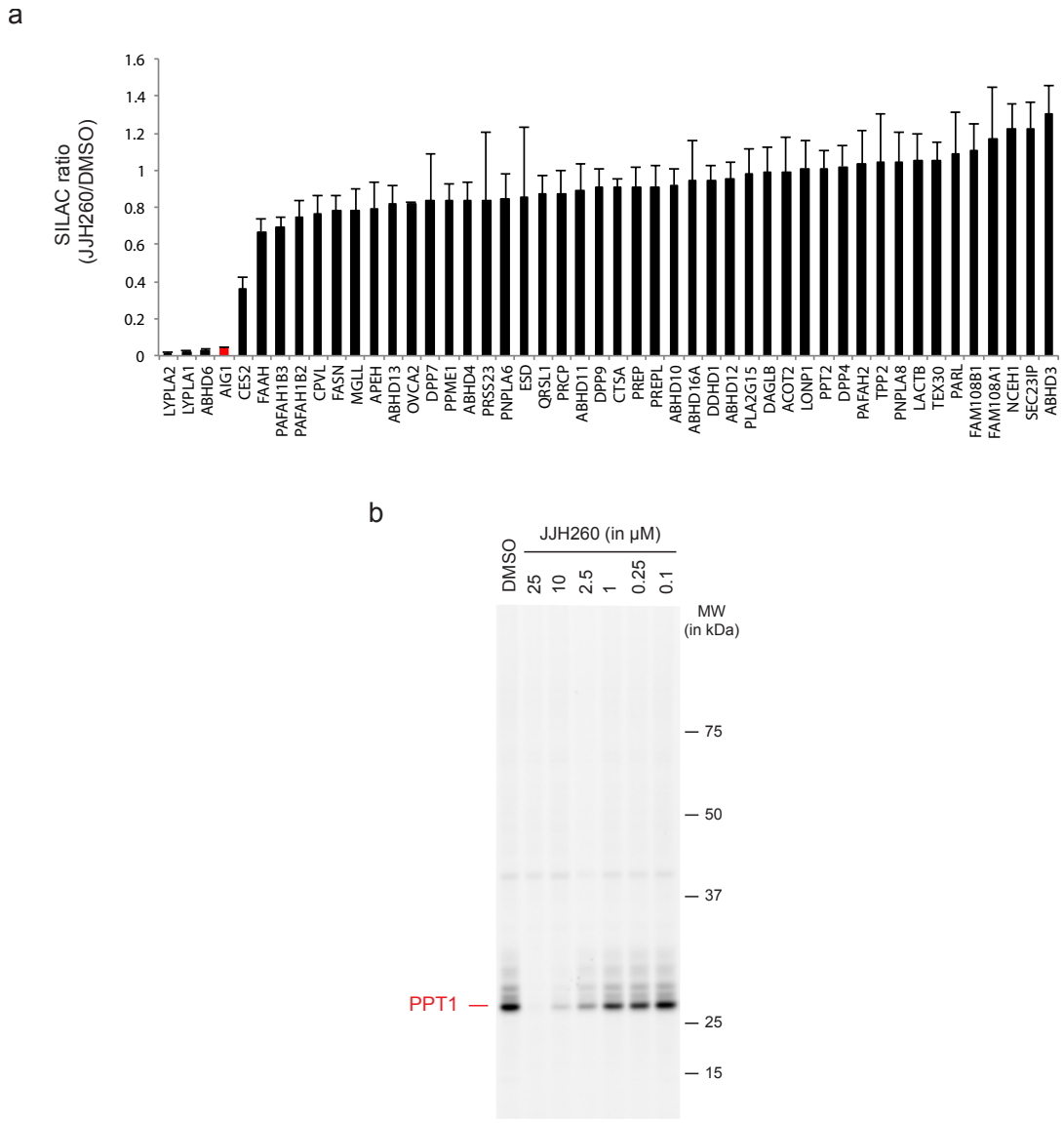

Supplementary Fig. 12. Competitive ABPP experiments to assess the selectivity of JJH260 against human Ser hydrolases. (**a**) Competitive ABPP-SILAC analysis to identify JJH260-inhibited proteins, where protein enrichment and inhibition were measured in SKOV3 cell proteomic lysates treated with DMSO or JJH260 (5 μM, 1 h) followed by FP-biotin (5 μM, 1 h) using established protocols[7]. Data represent the median SILAC ratios ± s. d. for peptides quantified for each protein from two biological replicates. (**b**) ABPP gel of the soluble fraction (1.0 mg proteome mL^{-1}) of PPT1-transfected HEK293T cells showing concentration-dependent inhibition with JJH260. Proteome was incubated with

the indicated concentration of JJH260 for 30 min at 23 °C, chased with 1 μM ABC45 for 30 min at 23 °C, treated with PNGase F, and then reacted with Rh-N_3 under standard click conditions and analyzed by SDS-PAGE and in-gel fluorescence scanning.

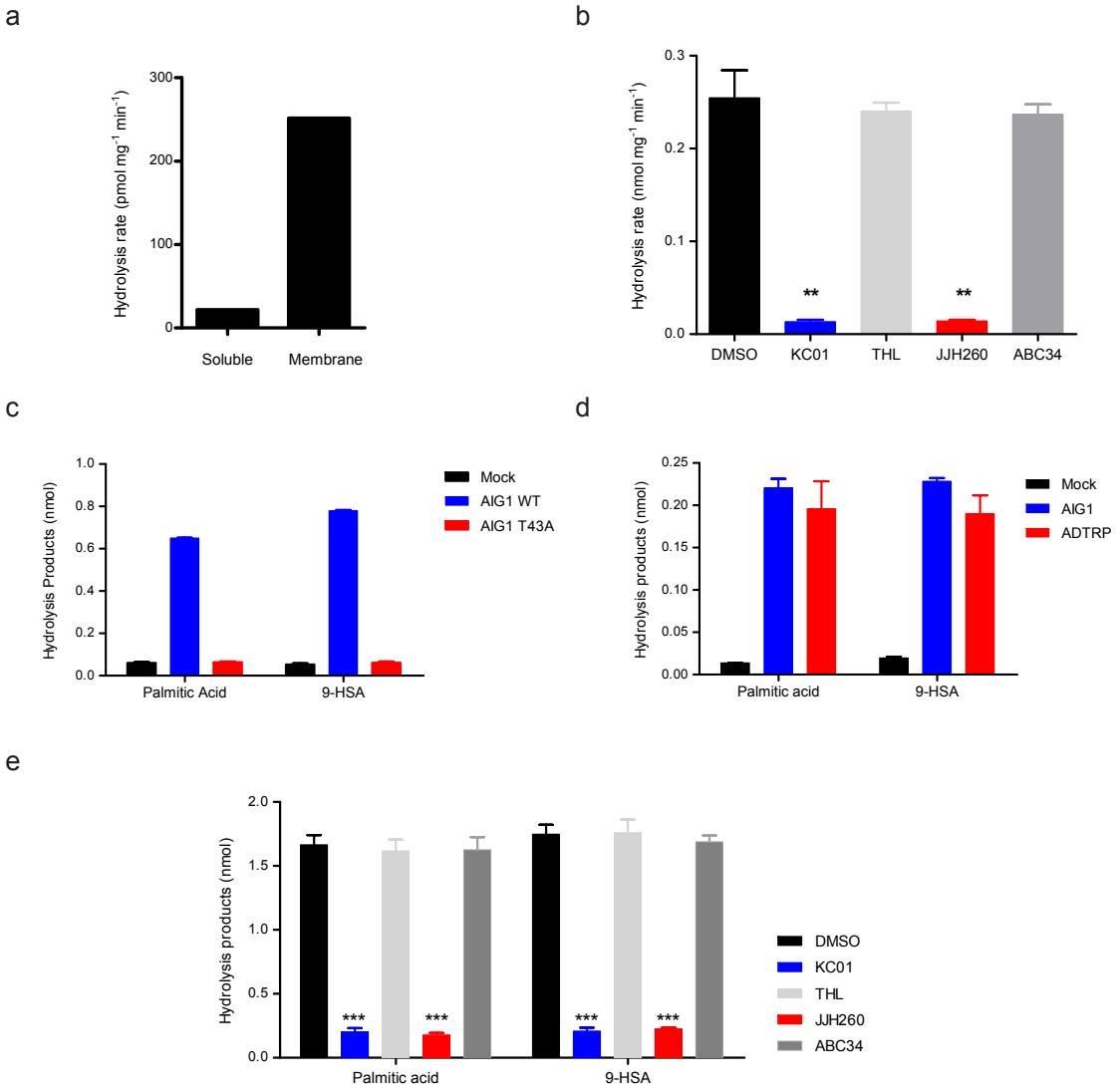

Supplementary Fig. 13. Further assessment of AIG1-dependent FAHFA hydrolysis in human cells. (**a**) *In vitro* 9-PAHSA hydrolysis assays for the membrane and soluble proteomes of LNCaP cells, showing that the majority of the hydrolytic activity resides in the membrane proteome. 20 µg of each proteome was incubated with 100 µM 9-PAHSA for 30 min at 37 °C. Data represent mean values for two biological replicates. (**b**) *In vitro* 9-PAHSA hydrolysis assays for the membrane proteome of LNCaP cells treated with DMSO or the indicated inhibitors (each at 5 µM, 30 min pre-treatment). 20

μg of each proteome was then incubated with 100 μM 9-PAHSA for 30 min at 37 °C. Data represent mean values ± s. e. m. for three biological replicates. $^{**}p < 0.01$ by Student's *t*-test for inhibitor-treated versus DMSO-treated controls. (**c**) $^{13}C,^{2}H$-PAHSA hydrolysis activity of HEK293T cells transfected with wild-type AIG1, the T43A-AIG1 mutant, or a mock control. Transfected cells were fed 2 μM $^{13}C,^{2}H$-PAHSA for 1 h. Data represent mean values ± s. e. m. for three biological replicates. (**d**) $^{113}C,^{2}H$-PAHSA hydrolysis activity of HEK293T cells transfected with wild-type AIG1, wild-type ADTRP, or a mock control. Transfected cells were fed a lower concentration of $^{13}C,^{2}H$-PAHSA (500 nM) for 1 h. Data represent mean values ± s. e. m. for three biological replicates. (e) $^{13}C,^{2}H$-PAHSA hydrolysis activity of hAIG1-transfected HEK293T cells treated *in situ* with DMSO or the indicated inhibitors (each at 5 μM, 4 h pre-treatment). Cells were fed 2 μM $^{13}C,^{2}H$-PAHSA for 1 h. Data represent mean values ± s. e. m. for four biological replicates. $^{***}p < 0.001$ by two-sided Student's *t*-test for inhibitor-treated versus DMSO-treated controls.

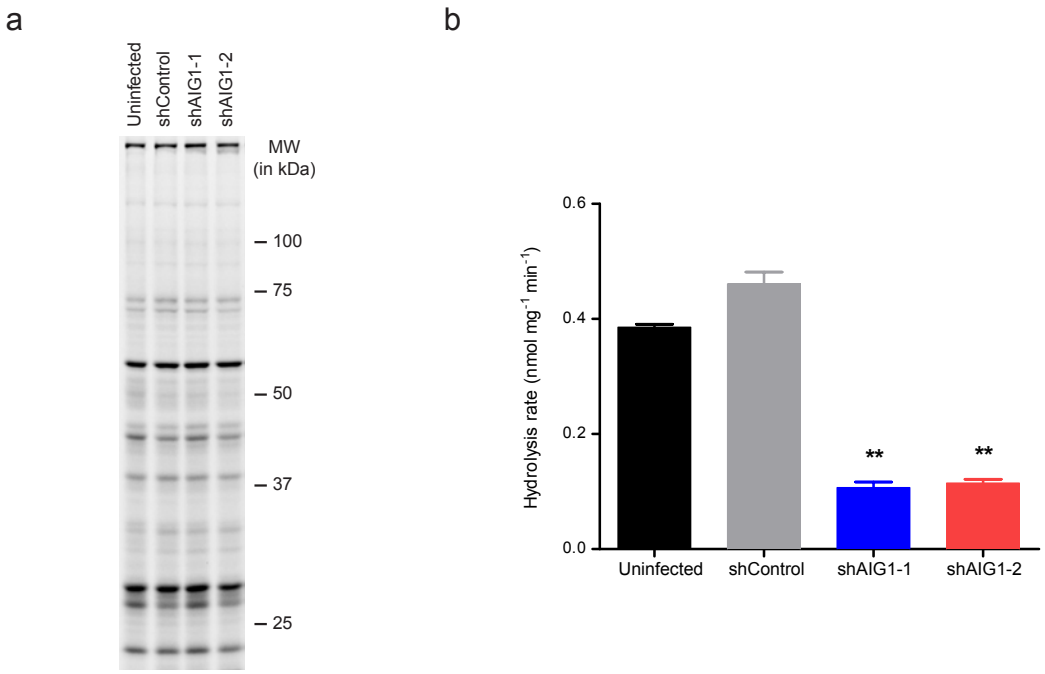

Supplementary Fig. 14. Further assessment of AIG1-knockdown human LNCaP cell lines. (**a**) ABPP gel of the membrane proteomes (1.0 mg proteome mL^{-1}) of the indicated shRNA cell lines. Proteomes were treated with 1 μM FP-Rh for 30 min at 37 °C and then analyzed by SDS-PAGE and in-gel fluorescence scanning. Note that global serine hydrolase signals are similar between shAIG1 and shControl cells (AIG1 is not detected with the FP-Rh probe in these cells due to overlapping serine hydrolase signals, but is shown in **Fig. 5d** using the WHP01 probe). (**b**) *In vitro* 9-PAHSA hydrolysis assays for the membrane proteomes of the indicated shRNA cell lines (shControl, shAIG1-1, and shAIG1-2) and an uninfected control LNCaP cell line. 20 μg of each proteome was incubated with 100 μM 9-PAHSA for 30 min at 37 °C. Data represent mean values ± s. e. m. for three biological replicates. $^{**}p < 0.01$ by two-sided Student's *t*-test for shAIG1 versus control cell lines.

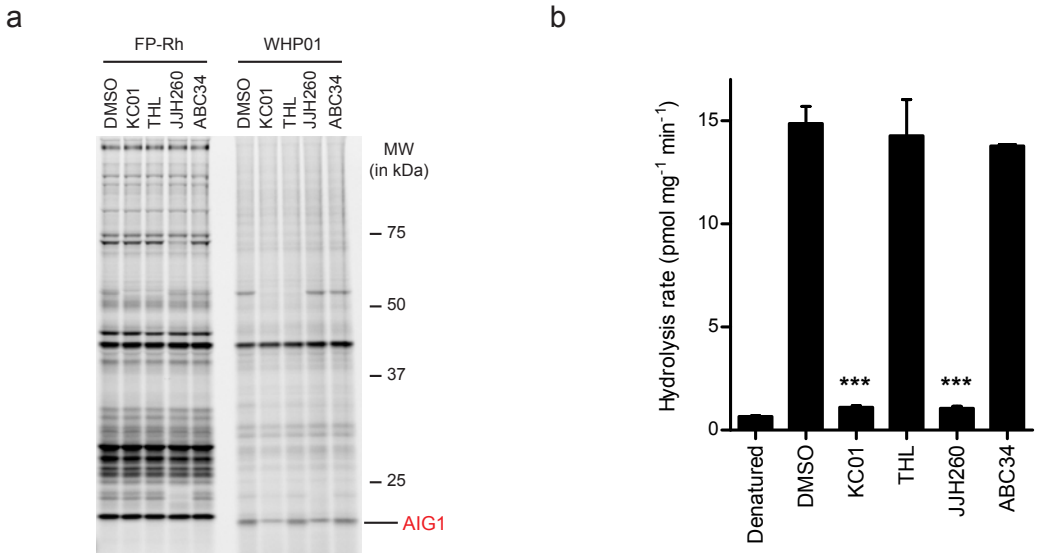

Supplementary Fig. 15. Further assessment of AIG1 and FAHFA hydrolysis in primary human T-cells. **(a**) ABPP gel of the membrane proteome (1.0 mg proteome mL^{-1}) of primary human T-cells treated with DMSO or inhibitors (each at 5 μM, 30 min, 37 °C). Proteomes were subsequently treated with either 1 μM FP-Rh or 2 μM WHP01 for 30 min at 37 °C and analyzed by SDS-PAGE and in-gel fluorescence scanning. The proposed band for AIG1 (partially obscured by an overlapping band) is indicated by a red label. (**b**) *In vitro* 9-PAHSA hydrolysis assays for the membrane proteomes of human T-cells treated with DMSO or inhibitors (each at 5 μM, 30 min pre-treatment). 20 μg of each proteome was incubated with 100 μM 9-PAHSA for 30 min at 37 °C. Data represent mean values ± s. e. m. for three biological replicates. ***$p < 0.001$ by two-sided Student's *t*-test for inhibitor-treated versus DMSO-treated controls.

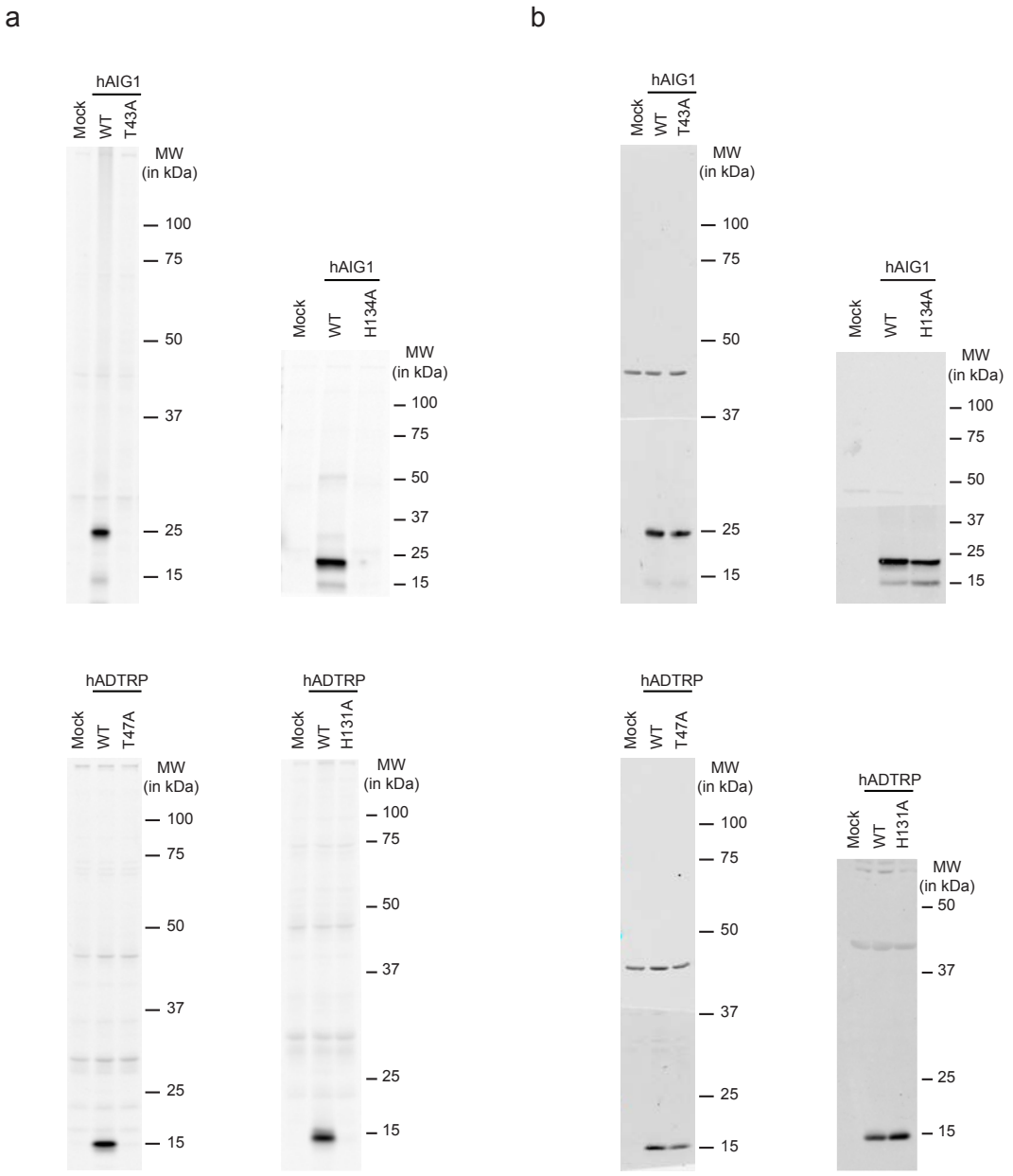

Supplementary Fig. 16. (**a**) Full gel images and (**b**) full Western blots for **Figures 2a-d**.

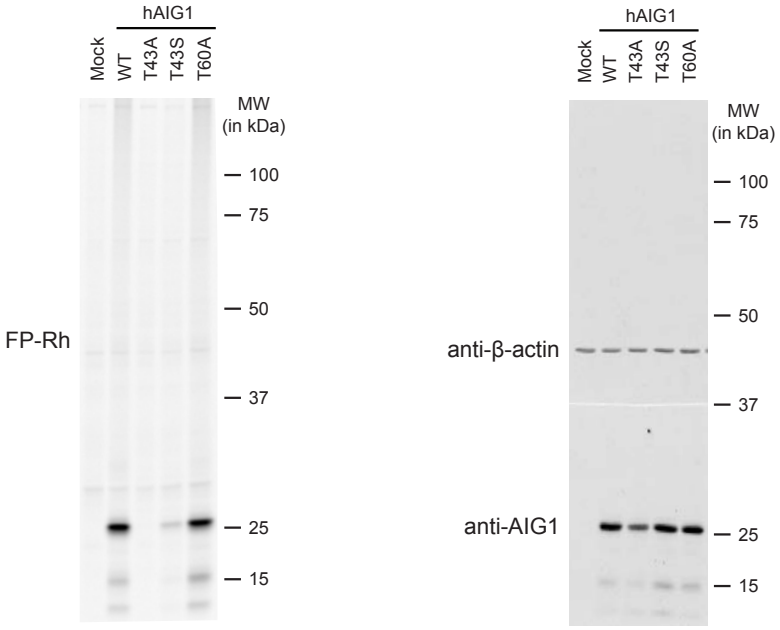

Supplementary Fig. 17. Full gel image and Western blot for **Figure 3c**.

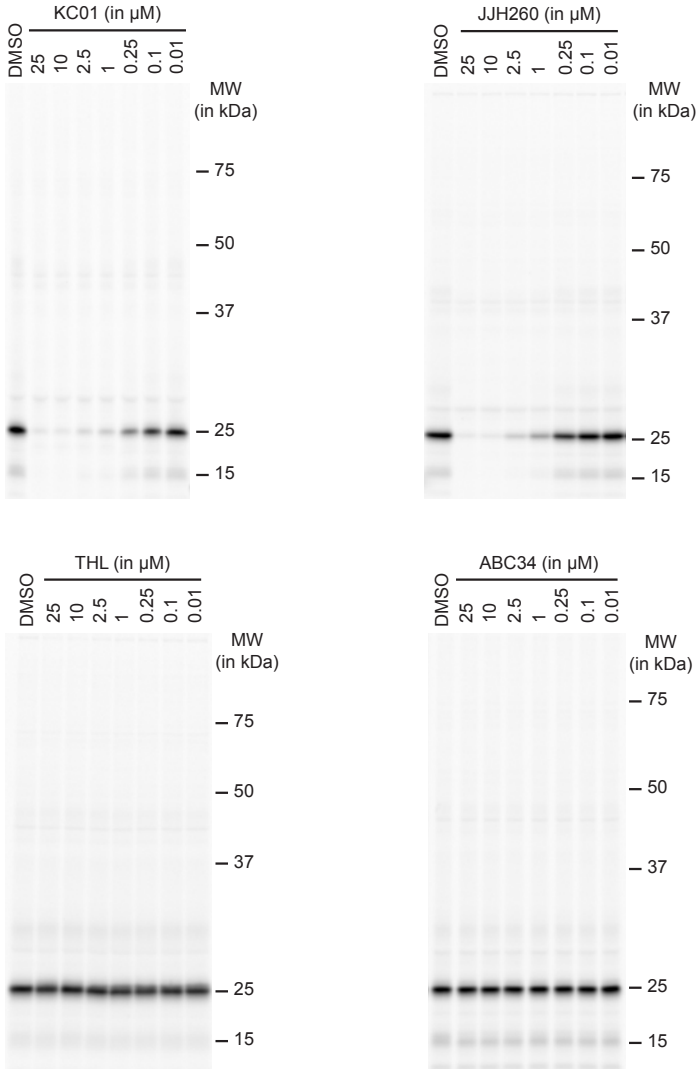

Supplementary Fig. 18. Full gel images for **Figure 4b**.

Supplementary Table 1. Complete ABPP-SILAC data sets. See attached Excel file.

Tab 1 ('FP-alkyne ratio SH'). SILAC ratios for serine hydrolases detected in the ABPP-SILAC analysis of SKOV3 cells treated *in situ* with 20 μM FP-alkyne for 1 h. The median ratios for each serine hydrolase detected in both biological replicates, as well as AIG1, are presented.

Tab 2 ('Probe-Probe control ratio SH'). SILAC ratios for serine hydrolases detected in a control experiment comparing proteins from heavy and light amino acid-labeled SKOV3 cell proteomes, each treated with FP-biotin (5 μM). The median ratios for each serine hydrolase detected in both biological replicates, as well as AIG1, are presented.

Tab 3 ('Probe-No Probe control ratio SH'). SILAC ratios for serine hydrolases detected in a control experiment comparing proteins from heavy amino acid-labeled SKOV3 cell proteome treated with FP-biotin (5 μM) with proteins from an untreated light amino acid-labeled SKOV3 cell proteome. The median ratios for each serine hydrolase detected in both biological replicates, as well as AIG1, are presented.

Tab 4 ('JJH260 ratio SH'). SILAC ratios for serine hydrolases detected in the ABPP-SILAC analysis of SKOV3 cell membrane proteome treated *in vitro* with 5 μM JJH260 for 1 h. The median ratios for each serine hydrolase detected in both biological replicates, as well as AIG1, are presented.

Tab 5 ('Summary JJH260 hits'). List of serine hydrolases inhibited by >50% in the ABPP-SILAC analysis of SKOV3 cell proteome treated *in vitro* with 5 μM JJH260 for 1 h.

Tab 6 ('Probe-Probe peptides all'). List of all peptides observed in a control experiment comparing proteins from heavy and light amino acid-labeled SKOV3 cell proteomes, each treated with FP-biotin (5 μM).

Tab 7 ('Probe-No Probe peptides all'). List of all peptides observed in a control experiment comparing proteins from heavy amino acid-labeled SKOV3 cell proteome treated with FP-biotin (5 μM) with proteins from an untreated light amino acid-labeled SKOV3 cell proteome.

Tab 8 ('FP-alkyne peptides all'). List of all peptides observed in an ABPP-SILAC analysis of SKOV3 cells treated *in situ* with 20 μM FP-alkyne for 1 h.

Tab 9 ('JJH260 peptides all'). List of all peptides observed in an ABPP-SILAC analysis of SKOV3 cell proteome treated *in vitro* with 5 μM JJH260 for 1 h.

For additional selectivity profiles for compounds used in this paper, please refer to Reference 5 (ABC34), Reference 6 (KC01), and Reference 8 (THL).

Supplementary Table 2. HHpred search results for AIG1/ADTRP alignment. See attached Excel file. The first tab shows filtered search results containing only those matches with E values < 0.1 and a predicted homologous region of amino acids that spans the conserved catalytic Thr residue of AIG1/ADTRP. The second tab contains the complete search output.

Mutation	Forward primer sequence
hAIG1	
S16A	5'-GATGGCAATCCTGCTGGCTTACTGCTCTATCCTGTG-3'
H32A	5'-CCATCGAAATGCCCTCAGCCCAGACCTACGGAGG-3’
T43A	5'-GGAGGGAGCTGGAAATTCCTGGCGTTCATTGATCTGG-3'
T43S	5'-GGAGGGAGCTGGAAATTCCTGTCGTTCATTGATCTGG-3'
T60A	5'-GGCATCTGTGTGCTGGCTGATCTTTCCAGTCTTCTGAC-3'
S63A	5'-GCTGACTGATCTTGCCAGTCTTCTGACTCGAGGAAGTGG-3'
S64A	5'-GCTGACTGATCTTTCCGCTCTTCTGACTCGAGGAAGTGG-3'
T67A	5'-CCAGTCTTCTGGCTCGAGGAAGTGGGAACCAGG-3'
S70A	5'-CTTCTGACTCGAGGAGCTGGGAACCAGGAGCAAGAGAGGC-3'
S84A	5'-GCTCAAGAAGCTCATCGCTCTCCGGGACTGG-3'
H134A	5'-GCTGAATCACGGAATGGCCACGACGGTTCTGCC-3’
T135A	5'-GCTGAATCACGGAATGCACGCGACGGTTCTGCC-3'
H150A	5’-GGACATCGCACGCTCAGTATCCCAGCAGGAGCAGC-3’
S154A	5'-CCATCAGTATCCCGCCAGGAGCAGCGGACTTACC-3'
S157A	5'-GTATCCCAGCAGGAGCGCCGGACTTACCGCC-3'
S166A	5'-CATATGTACCTTCGCTGTTGGCTATATATTATGGGTGTGCTGGG-3'
T180A	5'-GGTGCATCATGTAGCTGGCATGTGGGTGTACC-3'
S202A	5'-CAGGAGCCAGAATCATCTTCTTTGGGGCTACAACCATCTTAATG-3'
S227A	5'-CTGGGATACACAGAAAGCTATGGAAGAAGAGAAAGAAAAGCC-3'
hADTRP	
T47A	5'-GCAAGGTGGAAATATATGGCGCTGCTTAATCTGCTC-3'
H131A	5’-GGCTGAATCATGCAATGGCCACTTTCATATTCCCCATCAC-3’

Supplementary Table 3. Primers used for site-directed mutagenesis of hAIG1 and hADTRP.

Species detected	Precursor ion	Product ion	Collision energy	Dwell time	Polarity
[$^{13}C_{16}$]-PA-[D_{19}]-HSA	572.7	271.3	30	100	Negative
[$^{13}C_{16}$]-PAHSA	553.5	271.3	30	100	Negative
[D_{19}]-HSA	318.4	318.4	0	25	Negative
9-HHDA	285.2	285.2	0	25	Negative
[$^{13}C_{16}$]-PA	271.3	271.3	0	25	Negative
C17:1 FFA	267.2	267.2	0	25	Negative

Supplementary Table 4. Detailed MRM transitions used for the targeted LC-MS analysis.

References

1 Nomura, D. K. *et al.* Monoacylglycerol lipase regulates a fatty acid network that promotes cancer pathogenesis. *Cell* **140**, 49-61 (2010).

2 Adibekian, A. *et al.* Click-generated triazole ureas as ultrapotent in vivo-active serine hydrolase inhibitors. *Nat. Chem. Biol.* **7**, 469-478 (2011).

3 Ahn, K. *et al.* Discovery and characterization of a highly selective FAAH inhibitor that reduces inflammatory pain. *Chem. Biol.* **16**, 411-420 (2009).

4 Chang, J. W., Cognetta, A. B., 3rd, Niphakis, M. J. & Cravatt, B. F. Proteome-wide reactivity profiling identifies diverse carbamate chemotypes tuned for serine hydrolase inhibition. *ACS Chem. Biol.* **8**, 1590-1599 (2013).

5 Cognetta, A. B., 3rd *et al.* Selective *N*-Hydroxyhydantoin carbamate inhibitors of mammalian serine hydrolases. *Chem. Biol.* **22**, 928-937 (2015).

6 Kamat, S. S. *et al.* Immunomodulatory lysophosphatidylserines are regulated by ABHD16A and ABHD12 interplay. *Nat. Chem. Biol.* **11**, 164-171 (2015).

7 Adibekian, A. *et al.* Click-generated triazole ureas as ultrapotent *in vivo*-active serine hydrolase inhibitors. *Nature Chem. Biol.* **7**, 469-478 (2011).

8 Hoover, H. S., Blankman, J. L., Niessen, S. & Cravatt, B. F. Selectivity of inhibitors of endocannabinoid biosynthesis evaluated by activity-based protein profiling. *Bioorg. Med. Chem. Lett.* **18**, 5838-5841 (2008).

9 Yore, M. M. *et al.* Discovery of a class of endogenous mammalian lipids with anti-diabetic and anti-inflammatory effects. *Cell* **159**, 318-332 (2014).